doi.org/10.36721/PJPS.2025.38.4.REG.14233.1

# HPLC fingerprinting-guided determination of the optimal harvest period for Jinsi Huangju (*Chrysanthemum morifolium* Ramat.) and to elucidate its anti-inflammatory mechanisms

**Hualin Hu[1,2,4]* , Li Guo[1,2]* , Jian Fan[1,2], Fuxiao Wei[1,2], Xing Yu[3] and Jianguo Cen[4]**

[1]Natural Products Research Center of Guizhou Province, Guiyang, China
[2]State Key Laboratory of Discovery and Utilization of Functional Components in Traditional Chinese Medicine, Guizhou Medical University, Guiyang, China
[3]Guizhou Institute of Forest Inventory and Planning, Guiyang, China
[4]Guizhou Kangji Pharmaceutical Co., Ltd., Qiannan, China

**Abstract**: 'Jinsi Huangju' (JSHJ, *Chrysanthemum morifolium* Ramat.) is a medicinal plant traditionally used to manage inflammation. However, its optimal harvesting period and underlying anti-inflammatory mechanisms remain insufficiently explored. Therefore, this study aimed to investigate the effects of three JSHJ harvesting stages—initial flowering (CH), full flowering (SH), and final flowering (ZH)-on the bioactive compounds and to elucidate its anti-inflammatory mechanisms. The relative content of bioactive compounds (3,5-O-dicaffeoylquinic acid, chlorogenic acid, galuteolin) at each harvesting stage was determined using High-Performance Liquid Chromatography (HPLC, 1260, Agilent) fingerprints. The similarity of these fingerprints was then evaluated using the Chromatographic Fingerprint Similarity Evaluation System for Chinese Medicine (2004A edition). Anti-inflammatory activity was assessed in LPS-stimulated RAW 264.7 macrophages through MTT, Griess, and ELISA assays. The SH stage maximized JSHJ biomass and bioactive compounds. JSHJ extracts (20–50 μg/mL) significantly reduced LPS-induced levels of NO (from 9.45 to 0.16 μmol/L), TNF-α (from 127.26 to 8.09 pg/mL), and ROS. Among the extracts, petroleum ether (JSHJ-3) and ethyl acetate (JSHJ-4) exhibited the strongest anti-inflammatory effects.This study demonstrates that the SH stage is the most favorable harvest period for JSHJ, with extracts, particularly JSHJ-3/4, showing significant anti-inflammatory activity. These findings underscore the potential of JSHJ extracts as natural anti-inflammatory agents.

**Keywords**: Jinsi Huangju; HPLC fingerprint; harvesting stages; RAW 264.7; anti-inflammatory activity

*Submitted on 04-03-2025 – Revised on 07-04-2025 – Accepted on 17-04-2025*

## INTRODUCTION

'Jinsi Huangju' (JSHJ, *Chrysanthemum morifolium* Ramat.) is a member of the asteraceae family and is named for its petals, which resemble gold threads ("Jinsi" in Chinese). It is a popular herbal tea and has been consumed in China for centuries due to its health benefits (Chen *et al*., 2020). Its global economic significance arises from the diverse phytochemicals it contains, such as phenolic acids and flavonoids, which contribute to the production of medicinal teas, beverages, and seasonings (Yuan *et al*., 2020; Kim *et al*., 2022). Recent breeding efforts have focused on improving the yield of bioactive compounds, with JSHJ emerging as a premium cultivar due to its large flower size (up to 7 cm in diameter) and high brewing efficiency (Chen *et al*., 2020; Qin *et al*., 2020).

JSHJ quality is critically influenced by harvest timing, alongside cultivation practices and post-harvest processing (Qin *et al*., 2020; Bai *et al*., 2020). Among these, the timing of the harvest is particularly crucial for both the quantity and quality of the JSHJ. Optimal harvesting balances three metrics: biomass yield, bioactive compound levels (e.g., chlorogenic acid), and safety (Wang *et al*., 2020). For instance, in Atractylodes chinensis, harvest age significantly modulates atractylodin and organic acid concentrations (Liu *et al*., 2024). Similarly, the relative levels of volatile compounds with aromatic fragrances in Taiju markedly increased as the harvesting period was shortened (Yang *et al*., 2022). However, for JSHJ, the relationship between harvest stages-initial (CH), full (SH), and final flowering (ZH)-and bioactivity remains underexplored.

Previous studies have demonstrated that *C. morifolium* possesses a broad spectrum of pharmacological properties, such as antiviral, antibacterial, antioxidant, anti-inflammatory, and contributing to the prevention of chronic diseases (Yuan *et al*., 2020; Kim *et al*., 2022; Zhang *et al*., 2022;). Among these, phenolic acids, flavonoids, polysaccharides, and other active constituents are the key bioactive compounds (Chen *et al*., 2020; Ouyang *et al*., 2022; Fanaro *et al*., 2023; Al Mamun *et al*., 2024; Abotaleb *et al*., 2020). Interestingly, *C. morifolium* is primarily consumed as a hot-water infusion of its flowers in daily life (Li *et al*., 2019). While it has long been a

**Corresponding author:* e-mail: 366196832@qq.com,1358031333@qq.com

widely consumed health tea in China, the literature on the phytochemical composition and biological activities of JSHJ remains limited. In particular, Limited studies on JSHJ's anti-inflammatory activity in different solvents and optimal harvest time. Two key gaps remain in the current literature. First, previous studies have not systematically compared the chemical profiles across different harvest stages (CH/SH/ZH) using validated methods such as HPLC fingerprinting. Second, the anti-inflammatory effects of JSHJ extracts, particularly those obtained with different solvents, and the underlying mechanisms, such as the suppression of TNF-α and NO, have not been adequately characterized (Yang *et al*., 2022; Fanaro *et al*., 2023).

To address these gaps, this study aims to (1) establish HPLC fingerprints for JSHJ across harvest periods, (2) quantify key bioactive compounds, and (3) evaluate solvent-specific anti-inflammatory activity in vitro. This study bridges traditional knowledge and contemporary pharmacological standards by integrating phytochemical profiling with bioactivity validation, fostering the sustainable utilization of JSHJ in global health and wellness markets.

## MATERIALS AND METHODS

### *Reagents and materials*

Chromatographic-grade acetonitrile was purchased from Shanghai Titan Scientific Co. Ltd. (Shanghai, China). The murine macrophage cell line RAW 264.7 was acquired from ATCC (Rockville, MD, USA). lipopolysaccharide (LPS, *E. coli* 0111:B4), dimethyl sulfoxide (DMSO), and pyrrolidinedithiocarbamic acid (PDTC) were obtained via Sigma Chemical Co. Ltd. (St. Louis, MO, USA). Phosphate Buffered Saline (PBS) and 3-(4,5-dimethylthiazol-2-yl)-2,5-diphenyltetrazolium bromide (MTT) were sourced from Solarbio (Beijing, China). The reactive oxygen species (ROS) and nitric oxide (NO) assay kit were sourced from Beyotime (Shanghai, China). Tumor necrosis factor-α (TNF-α, cat. EK0527) was bought from Boster (Wuhan, China). All other chemicals and solvents were of analytical grade and applied directly without additional purification. Reference samples, including chlorogenic acid (B20782, ≥98%), galuteolin (DM0016-0020, ≥98%), and 3,5-O-dicaffeoylquinic acid (DY0036-0020, ≥98%), were supplied by Shanghai Yuanye Bio-Technology Co. Ltd. (Shanghai, China) and Chengdu Desite Bio-Technology Co. Ltd. (Chengdu, China).

JSHJ was sourced from the *Chrysanthemum* planting base in Yunwu Town, Guiding County, Guizhou Province, China. The samples were confirmed as the dried flower heads of JSHJ by Professor Long Qingde from Guizhou Medical University. Collection occurred between mid-October and mid-November 2023, and the samples were categorized into three stages based on the flowering period: initial flowering (CH), full flowering (SH), and final flowering (ZH) (Fig. 1). Additionally, samples from each flowering stage were further divided into three parts: mixed parts (1), non-green parts (2), and green parts (3). All JSHJ plants were grown in the same garden under uniform conditions. Three biological repetitions were obtained for each harvest period.

### *Determination of biomass*

Forty dried flowers of JSHJ from each period were randomly selected, accurately weighed using an analytical balance (ME103E, Mettler Toledo, Switzerland), and recorded. Three batches of each sample were measured.

### *Determination of HPLC fingerprint*

*Preparation of the experimental and standard solution*

The JSHJ samples were ground, sieved through a 20-mesh sieve, and accurately weighed (0.25 g) into a 50-mL *stoppered conical flask.* After adding 25 mL of 70% methanol, ultrasonic extraction (300 W, 45 kHz, 40 min) was performed. The solution was replenished with 70% methanol to the initial weight, vigorously shaken, and filtered through a 0.45 μm microporous membrane. The filtrate was collected as the test solution. The weight of 3,5-O-dicaffeoylquinic acid, galuteolin, and chlorogenic acid were precisely measured and moved into a 10-mL brown glass volumetric flask. Thereafter, a 70% methanol solvent was incorporated to make up mixed standard solutions with concentration values of 0.080, 0.025, and 0.035 mg/mL.

### *Chromatographic parameters for HPLC*

The analysis was conducted using a HPLC (1260, Agilent, USA) fitted utilizing a COSMOSIL C18 column (4.6 mm × 250 mm, 5 μm). To improve separation process and ensure stable peak profiles, the parameters were slightly modified based on the Chinese Pharmacopoeia (2020 edition). Acetonitrile served as solvent A in the mobile phase, while a 0.1% aqueous phosphoric acid solution was employed as solvent B. The mobile phase system was operated at 0.8 mL/min flow rate, with the column temperature set to 30°C as per the DAD settings, and detection at a wavelength of 348 nm. A 10 μL injection volume was used, and the gradual elution parameters are outlined in table 1. Through systematic methodological verification, including experiments on precision, repeatability, stability, and correlation coefficient, it was confirmed that the key parameters meet the analytical standards. The precision relative standard deviation (RSD) was 2.82%, the stability RSD was 3.87%, the repeatability RSD was 4.01%, and the correlation coefficient ($R^2$) was 0.9996.

### *Formation and similarity analysis of HPLC fingerprints*

The JSHJ samples were examined at nine distinct time points and from various parts using optimized chromatographic settings. The generated HPLC fingerprints were subsequently transferred into the

Chromatographic Fingerprint Similarity Evaluation System for Chinese Medicine (2004A edition). The median approach was employed to determine the ideal time window width of 0.6 minutes. Multi-point fitting procedure was performed, followed by automatic peak alignment and the creation of control charts to examine the consistency of chromatographic peaks across the nine groups.

***Evaluation of anti-inflammatory activities***

*Preparation of JSHJ extracts*

According to the findings in biomass and relative content of bioactive compounds, the SH phase was selected as the research subject for studying the anti-inflammatory activity of JSHJ samples. The JSHJ samples were subsequently crushed into a fine dust, sieved via a 20-mesh filter, and stored in airtight containers. Following this, the samples were extracted using both ultrasonic and water bath methods, with each extraction repeated three times using the following solvents:

***Water Extraction (JSHJ-1 and JSHJ-2)***

Weigh 21.2 mg JSHJ powder → Add to Erlenmeyer flask + 25 mL deionized water → Shake thoroughly →Water bath heat at 80°C for 3 h → Filter → Concentrate filtrate via rotary evaporation at 70°C → Obtain JSHJ-1.

Weigh 20.6 mg JSHJ powder → Add to Erlenmeyer flask + 25 mL deionized water → Shake thoroughly →Soak for 20 min → Ultrasonicate (40 kHz, 45°C) for 30 min → Filter → Concentrate filtrate at 70°C → Obtain JSHJ-2.

***Petroleum Ether Extraction (JSHJ-3)***

Weigh 23.1 mg JSHJ powder → Add to Erlenmeyer flask + 25 mL petroleum ether → Shake thoroughly →Ultrasonicate (40 kHz, 45°C) for 30 min→ Filter and concentrate → Obtain JSHJ-3.

***Ethyl Acetate Extraction (JSHJ-4)***

Weigh 21.7 mg JSHJ powder → Add to Erlenmeyer flask + 25 mL ethyl acetate → Shake thoroughly →Ultrasonicate (40 kHz, 45°C) for 30 min→ Filter and concentrate → Obtain JSHJ-4.

***80% Ethanol Extraction (JSHJ-5 and JSHJ-6)***

Weigh 22.0 mg JSHJ powder → Add to Erlenmeyer flask + 25 mL 80% ethanol → Shake thoroughly →Water bath heat at 80°C for 3 h → Filter and concentrate → Obtain JSHJ-5.

Weigh 21.9 mg JSHJ powder → Add to Erlenmeyer flask + 25 mL 80% ethanol → Shake thoroughly →Ultrasonicate (40 kHz, 45°C) for 30 min→ Filter and concentrate → Obtain JSHJ-6.

***Cell cultivation***

The RAW 264.7 cells were maintained in Dulbecco's Modified Eagle's Medium (Gibco, Carlsbad, USA), with the addition of 100 U/mL penicillin/streptomycin (Servicebio, Wuhan, China) and 10% fetal bovine serum (Biological Industries, Israel). The cells were kept in a 37°C incubator with 5% $CO_2$, with regular medium changes and subculturing, and were cultured until reaching the logarithmic phase for subsequent experiments.

***Cellular viability measurement***

The impact of JSHJ extracts in different solvents on RAW 264.7 cells was evaluated using the MTT test. In brief, cells were plated at a density of $2.0 \times 10^4$ cells per well in 96-well plates. 24 h later, the cells were incubated with 2, 20, or 50μg/mL extracts for another 24 h. PBS served as the untreated control. Subsequently, 20μL of the MTT working solution (0.5 mg/mL) was introduced, and the cells were maintained at 37°C for 4 h. The formazan crystals were subsequently solubilized in 50μL of Triple liquid. The absorbance of the solution was recorded utilizing a plate reader (BioTek, USA) at 570 nm.

***NO production measurement***

The NO production within the growth broth was measured utilizing a NO detection kit in accordance with the Griess assay. $2.0 \times 10^4$ RAW 264.7 cells per well were placed into 96-well plates and treated previously with 2, 20, or 50 μg/mL extracts for 2 h, then treated with 1 μg/mL LPS. After incubating for 20 h, the same amount of Griess reagent was added to the culture supernatant. The mixture's absorbance was determined utilizing a plate reader at 540 nm.

***Determinations of TNF-α levels***

$2.0 \times 10^4$ RAW 264.7 cells per well were plated into 96-well plates and pretreated with 2, 20, or 50μg/mL extracts for 2 h, then treated with 1μg/mL LPS. After incubating for 20 h, TNF-α levels in the supernatant were determined utilizing the specific ELISA kits, in accordance with the manufacturer's protocol.

***Measurement of ROS in Intracellular***

Intracellular ROS generation was quantified utilizing the DCFH-DA fluorescent dye, as described in previous studies (Xiong *et al*., 2022; Li *et al*., 2021). Due to its non-polar nature, DCFH-DA easily penetrates the cell membrane and is hydrolyzed by intracellular esterases to yield DCFH, which stays within the cells. The oxidation of DCFH leads to the formation of the fluorescent compound 2,7-dichlorofluorescein, which can be quantified using the High Content Screening Studio™ (Thermo Fisher Scientific, USA). For this experiment, RAW 264.7 cells were cultured in 96-well plates at a concentration of $2 \times 10^4$ cells per well, pretreated with 2, 20, or 50 μg/mL extracts for 2 h, then treated with 1 μg/mL LPS. After incubating for 20 h, the cells were incubated in the presence of 10 μM DCFH-DA and DAPI for 30 minutes at 37°C under dark conditions. After the incubation step, cells underwent three washes with PBS, and 50 μL of PBS was subsequently added. The samples underwent analysis using High Content Screening.

**Table 1**: Protocol for gradient elution.

| Time (min) | Mobile phase A (%) | Mobile phase B (%) |
|---|---|---|
| 0 | 10 | 90 |
| 11 | 18 | 82 |
| 30 | 20 | 80 |
| 62 | 20 | 80 |

**Table 2**: Results of biomass determination for JSHJ samples

| samples | Biomass/g | | | |
|---|---|---|---|---|
| | 1 | 2 | 3 | Mean ± SD |
| CH | 17.43 | 17.82 | 17.07 | 17.44±0.38** |
| SH | 26.37 | 24.18 | 25.00 | 25.18±1.11 |
| ZH | 11.85 | 12.07 | 11.83 | 11.92±0.13** |

Note: Comparison between each group and SH **$P$<0.01.

**Table 3**: Similarity analysis of JSHJ samples HPLC fingerprint

| samples | CH-I | CH-2 | CH-3 | SH-I | SH-2 | SH-3 | ZH-I | ZH-2 | ZH-3 | R |
|---|---|---|---|---|---|---|---|---|---|---|
| CH-1 | 1.000 | | | | | | | | | |
| CH-2 | 0.989 | 1.000 | | | | | | | | |
| CH-3 | 0.639 | 0.535 | 1.000 | | | | | | | |
| SH-1 | 0.999 | 0.990 | 0.636 | 1.000 | | | | | | |
| SH-2 | 0.986 | 0.993 | 0.525 | 0.983 | 1.000 | | | | | |
| SH-3 | 0.647 | 0.541 | 0.998 | 0.644 | 0.533 | 1.000 | | | | |
| ZH-1 | 0.997 | 0.995 | 0.605 | 0.998 | 0.985 | 0.613 | 1.000 | | | |
| ZH-2 | 0.989 | 0.999 | 0.529 | 0.990 | 0.992 | 0.537 | 0.995 | 1.000 | | |
| ZH-3 | 0.628 | 0.522 | 0.988 | 0.628 | 0.509 | 0.992 | 0.599 | 0.521 | 1.000 | |
| R | 0.997 | 0.996 | 0.600 | 0.998 | 0.987 | 0.608 | 1.000 | 0.996 | 0.592 | 1.000 |

**Table 4**: Relative retention time of common peak

| samples | Relative retention time of common peak | | | | | | |
|---|---|---|---|---|---|---|---|
| | P1 | P2 | P3 | P4 | P5 | P6 | P7 |
| CH-1 | 0.366 | 0.693 | 0.768 | 0.922 | 1.000 | 1.074 | 1.206 |
| CH-2 | 0.357 | 0.695 | 0.769 | 0.923 | 1.000 | 1.076 | 1.206 |
| CH-3 | 0.343 | 0.693 | 0.820 | 0.922 | 1.000 | 1.081 | 1.220 |
| SH-1 | 0.342 | 0.694 | 0.769 | 0.923 | 1.000 | 1.077 | 1.207 |
| SH-2 | 0.338 | 0.693 | 0.768 | 0.922 | 1.000 | 1.078 | 1.210 |
| SH-3 | 0.322 | 0.689 | 0.767 | 0.922 | 1.000 | 1.079 | 1.223 |
| ZH-1 | 0.320 | 0.688 | 0.766 | 0.922 | 1.000 | 1.078 | 1.213 |
| ZH-2 | 0.320 | 0.688 | 0.766 | 0.922 | 1.000 | 1.078 | 1.212 |
| ZH-3 | 0.321 | 0.689 | 0.767 | 0.921 | 1.000 | 1.079 | 1.222 |

**Table 5**: Relative peak area of common peak

| samples | Relative peak area of common peak | | | | | | |
|---|---|---|---|---|---|---|---|
| | P1 | P2 | P3 | P4 | P5 | P6 | P7 |
| CH-1 | 0.408 | 0.035 | 0.461 | 0.094 | 1.000 | 0.620 | 1.797 |
| CH-2 | 0.444 | 0.029 | 0.590 | 0.106 | 1.000 | 0.921 | 2.159 |
| CH-3 | 0.567 | 0.107 | 0.120 | 0.084 | 1.000 | 0.195 | 0.610 |
| SH-1 | 0.357 | 0.026 | 0.444 | 0.098 | 1.000 | 0.576 | 1.653 |
| SH-2 | 0.534 | 0.061 | 1.040 | 0.136 | 1.000 | 1.278 | 3.128 |
| SH-3 | 0.506 | 0.094 | 0.129 | 0.114 | 1.000 | 0.182 | 0.631 |
| ZH-1 | 0.323 | 0.026 | 0.412 | 0.099 | 1.000 | 0.632 | 1.646 |
| ZH-2 | 0.322 | 0.020 | 0.581 | 0.093 | 1.000 | 0.902 | 2.108 |
| ZH-3 | 0.370 | 0.086 | 0.148 | 0.059 | 1.000 | 0.176 | 0.516 |


**Fig.1**: JSHJ samples from different harvesting periods.

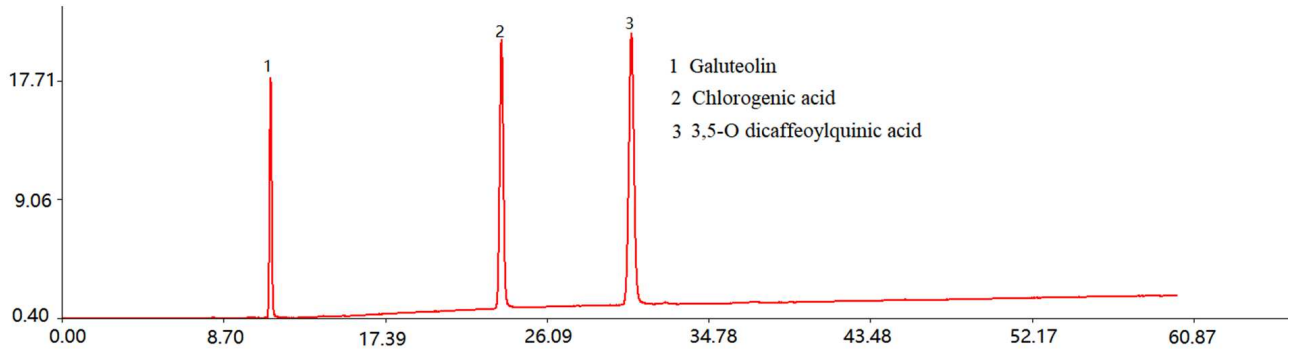


**Fig. 2**: HPLC profile of mixed reference substance

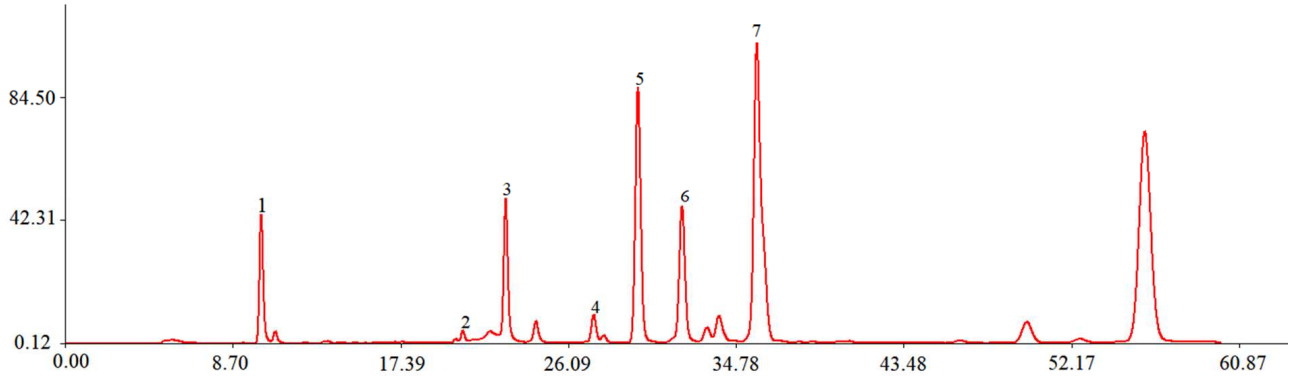


**Fig. 3**: HPLC fingerprint common peak of JSHJ samples. (1) Chlorogenic acid. (3) Galuteolin. (5) 3,5-O-dicaffeoylquinic acid

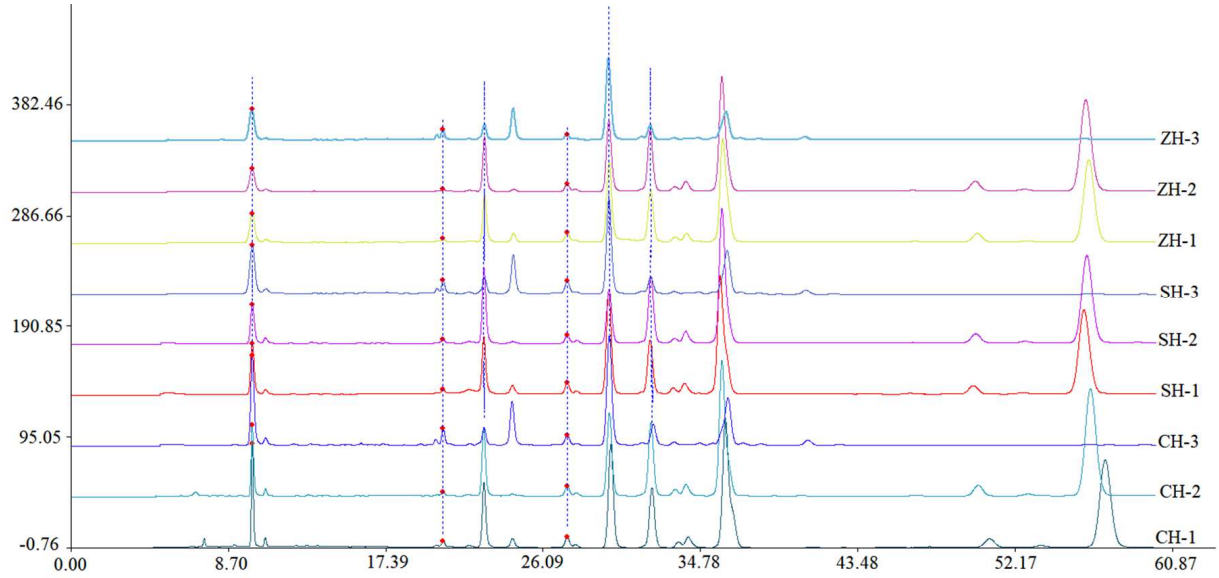


**Fig. 4**: HPLC spectrum of ethanol extract of JSHJ samples

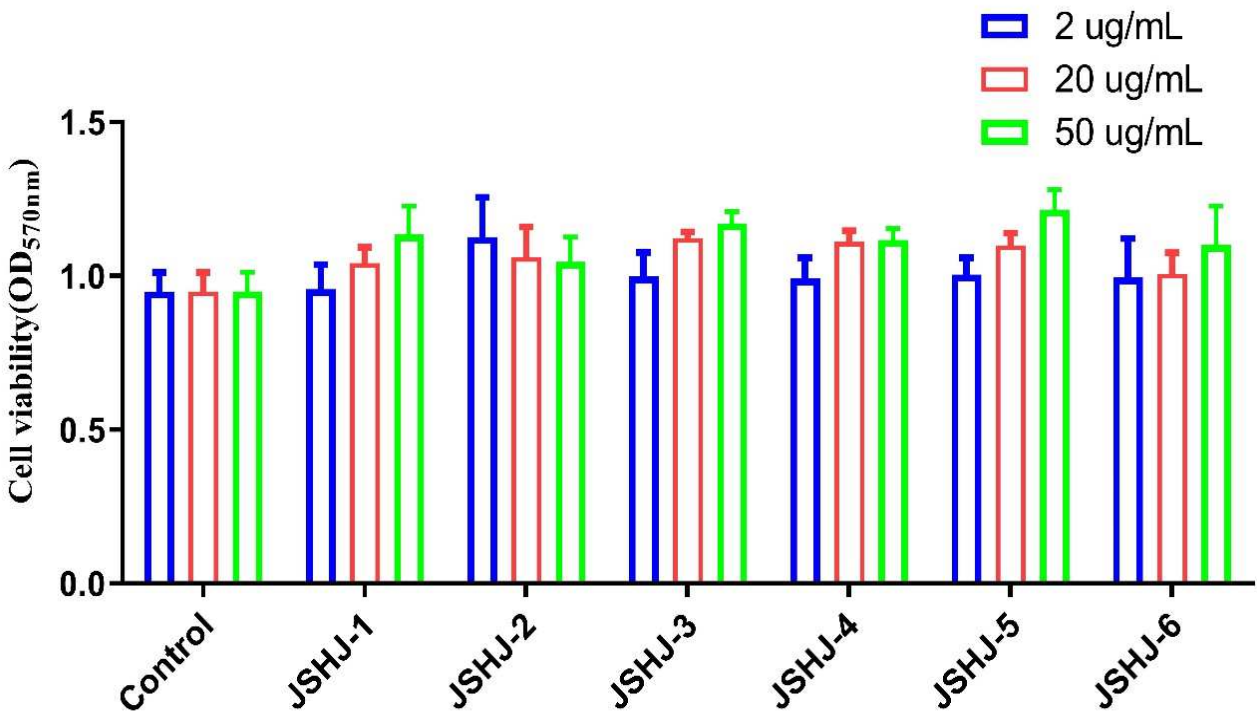


**Fig. 5**: Effects of JSHJ on cell viability in RAW 26.47 macrophage cells. Bar graphs represent data from three independent experiments. Each value is presented as the mean ± SD (n = 3).

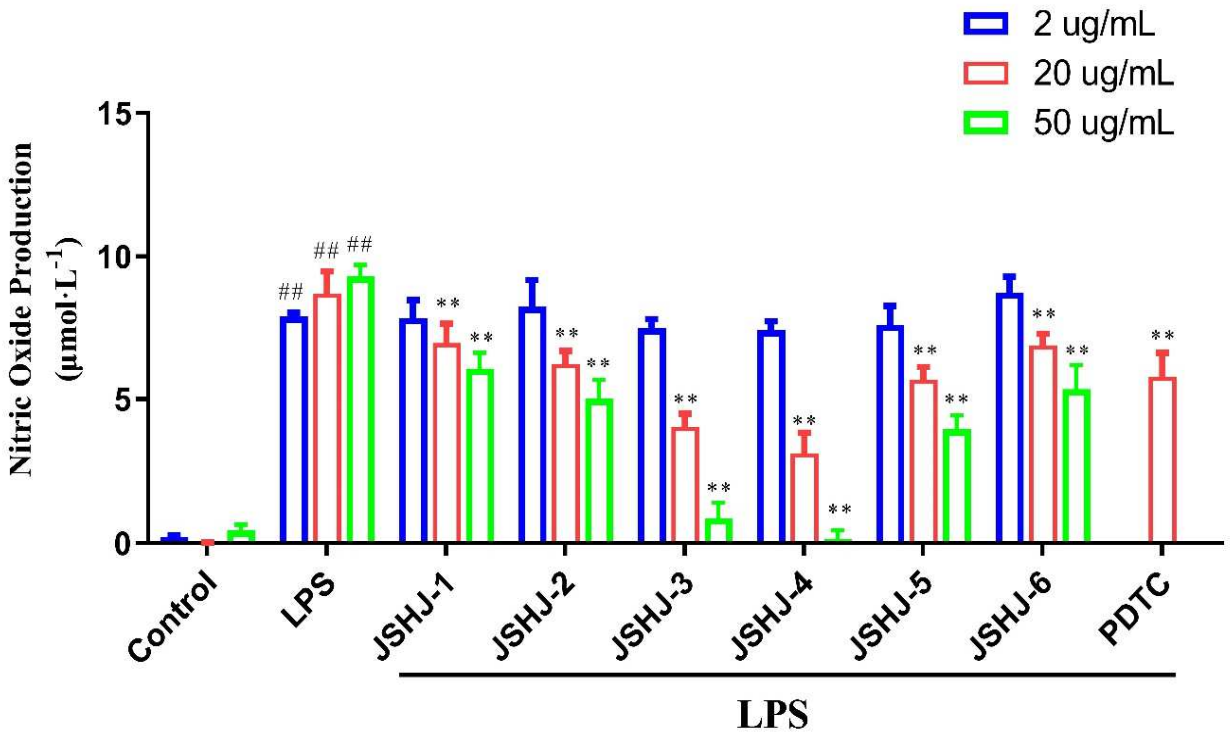


**Fig. 6**: Effects of JSHJ on NO production in RAW 264.7 macrophage cells treated with LPS. Data are presented as the mean ± SD (n = 3). $^{\#\#}P<0.01$vs. the control group, $^{**}P<0.01$ vs. the treatment with LPS alone.

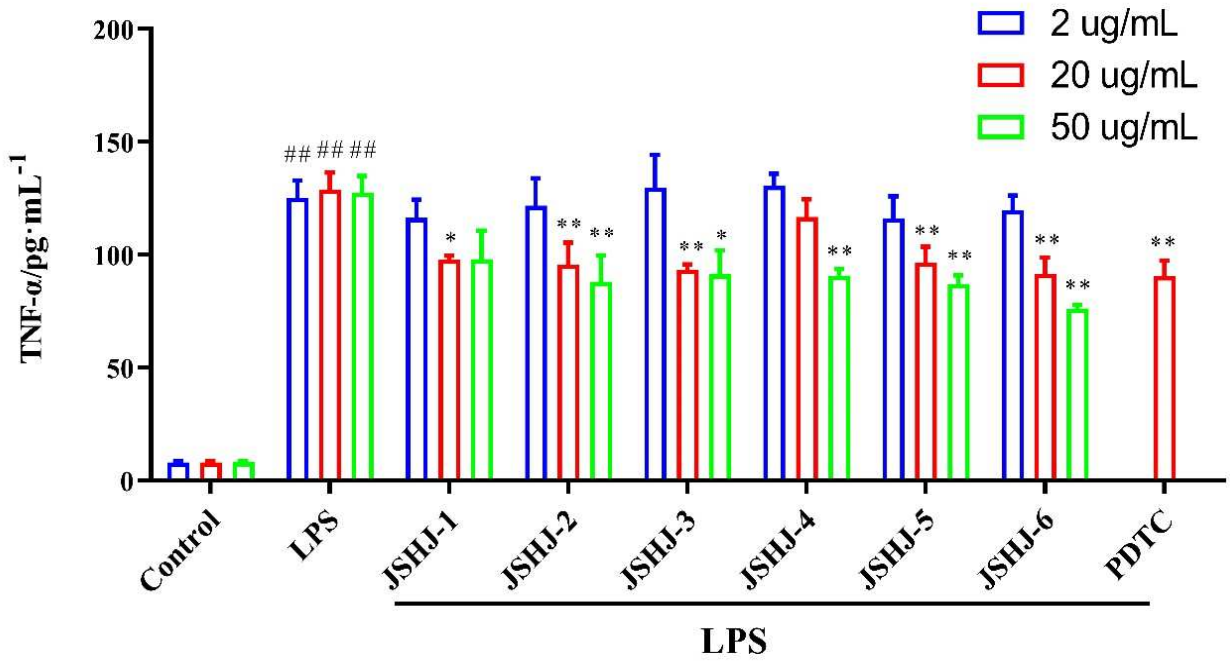


**Fig. 7**: Effect of JSHJ extract (2, 20, and 50 μg/mL) on LPS-induced proinflammatory cytokine production in RAW 264.7 cells. Data are presented as the mean ± SD (n = 3). $^{\#\#}P<0.01$vs. the control group, $^{**}P<0.01$ and $^{*}P<0.01$ vs. the treatment with LPS alone.

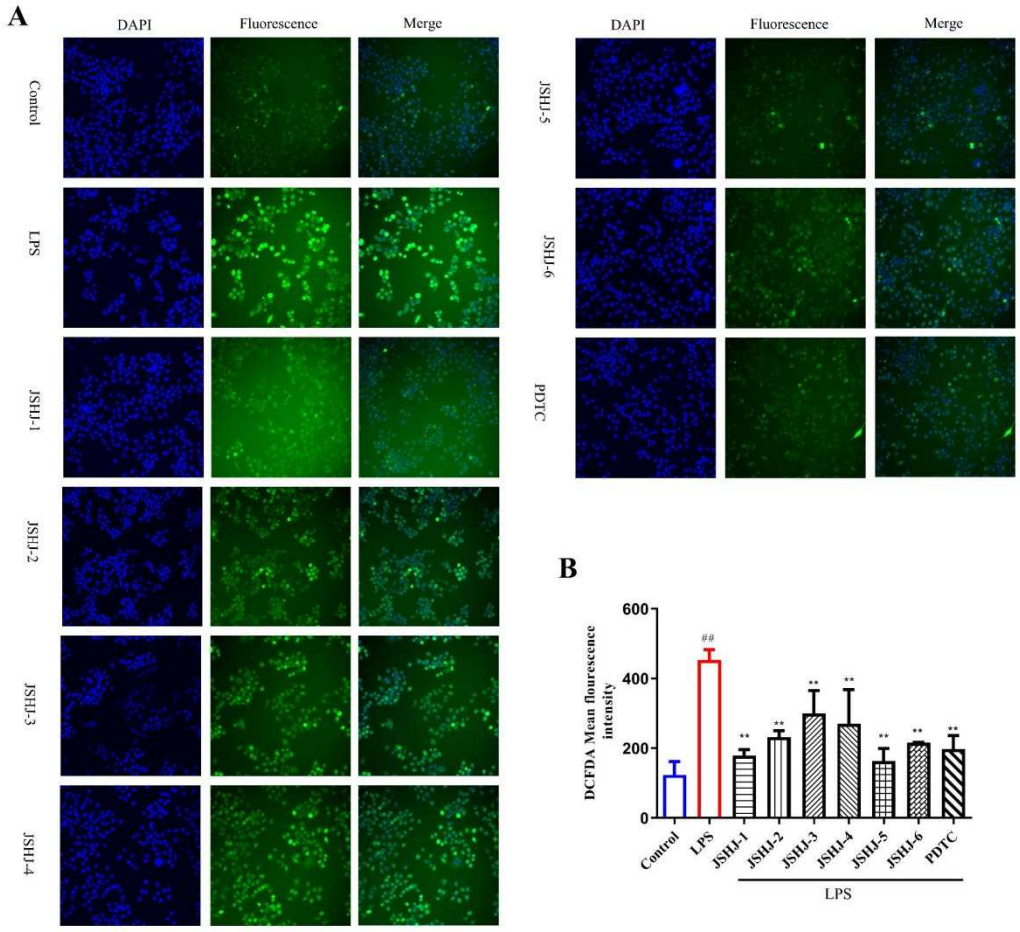


**Fig. 8**: Effect of JSHJ extract (50 µg/mL) on LPS-induced ROS production in RAW 264.7 cells.
(A) ROS fluorescence detection images by DCFH-DA processing. (B) Quantitative analysis of ROS fluorescence. Each value represents the mean ± SD (n = 3). $^{\#\#}P<0.01$vs. the control group, $^{**}P<0.01$ and $^{*}P<0.01$ vs. the treatment with LPS alone.

## STATISTICAL ANALYSIS

Each experiment included at least three biological replicates. Data were analyzed using IBM SPSS Statistics 19 (IBM, USA), and results are presented as mean ± standard deviation (SD). The Least Significant Difference (LSD) test was used to assess statistical significance (*$P$ < 0.05 and **$P$ < 0.01). Graphs were generated using GraphPad Prism version 8.0 (San Diego, CA).

## RESULTS

### *Biomass of JSHJ*

The results showed that the biomass of JSHJ increased from CH to SH, reaching its maximum value at SH ($P$ < 0.01). From SH to ZH, plant growth transitioned from full bloom to decline, with metabolite consumption exceeding accumulation. This, along with factors such as falling petals, led to a gradual decrease in biomass. The biomass ranking for the same number of plants was SH (25.18 ± 1.11 g) > CH (17.44 ± 0.38 g) > ZH (11.92 ± 0.13 g), as detailed in table 2.

### *HPLC profiles of the standard and JSHJ samples*

Both the standard and tested solutions were analyzed with the chromatographic parameters described in Table 1, producing their respective HPLC chromatograms, as shown in Fig. 2 and Fig. 3. By analyzing the reference product's chromatogram alongside three other reference samples, peaks 1, 2, and 3 were found to correspond to

chlorogenic acid, galuteolin, and 3,5-O-dicaffeoylquinic acid in the mixed reference samples (Fig. 2).Taking into account the elution profiles and peak areas of these three separation peaks in the standard solution, we proposed that peaks No. 1, 3, and 5 in the JSHJ sample represent chlorogenic acid, galuteolin, and 3,5-O-dicaffeoylquinic acid, respectively. However, as a result of interference from unrelated peaks in the JSHJ samples, a slight forward movement in the positions of peaks No. 1, 3, and 5 was seen.

***Formation of HPLC fingerprint and similarity analysis of JSHJ***

Under the specified chromatographic conditions, the chromatograms of nine JSHJ batches were recorded in succession and subsequently imported into Software System. The SH-1 chromatogram was used as a reference to calculate the 0.6-minute time window width, determined using the median approach. Multi-point correction was applied, and the chromatographic peaks were automatically matched, resulting in the generation of reference maps. Through chromatographic peak matching, seven characteristic peaks were successfully identified. Using the full-wavelength scanning map from the DAD, and by comparing it with the reference substances, one component was identified as 3,5-O-dicaffeoylquinic acid (P5). Peak 5 was chosen as the reference peak to calculate the similarity between the nine groups of JSHJ samples.

The feature map overlay is presented in fig. 4, with the similarity analysis results shown in table 3.

According to the SH-1 map (fig. 4), a total of seven common peaks were identified. Three components were confirmed by comparison with the control substance (fig. 2). The types of chemical constituents in the JSHJ samples were similar across different harvesting periods. However, the chemical composition varied between different plant parts within the same harvest period, particularly between the green and non-green parts. Notably, the green parts showed no absorption peak around 57 minutes, in contrast to the mixed and non-green parts. The results from the similarity evaluation can be found in table 3. The similarity between the JSHJ samples from the nine lots and the control atlas ranged from 0.592 to 1.000. Further analysis revealed that the green part had a low similarity, while the non-green part exhibited a high similarity, closely resembling the mixed part. Additionally, the green parts showed consistent absorption peaks throughout the study, except at the 57-minute mark. This suggests that the green parts may have potential for development and utilization, as indicated by the HPLC chromatogram.

Based on the chemical composition, 3,5-O-dicaffeoylquinic acid was found to have the largest and most stable peak area, and therefore, it was selected as the internal standard peak (P5). The relative retention times of each common peak are provided in table 4. Using the peak area of 3,5-O-dicaffeoylquinic acid as a reference, The peak area ratios for each common peak were calculated and are presented in table 5. Among these, the peak areas of P1 (chlorogenic acid), P3 (galuteolin), P4, P5 (3,5-O-dicaffeoylquinic acid), P6, and P7 were larger. According to the areas of the common peaks, the relative content at SH was higher, with a trend of
SH > CH > ZH.

***Toxicity assessment of JSHJ extract on RAW264.7 Cells***

To analyze the cytotoxicity of JSHJ extract on RAW 264.7 macrophage-like cells, a standard cell viability measurement was conducted. The cytotoxicity of the JSHJ extract on RAW264.7 cells was assessed using the MTT test. The data from the toxicity test are shown in fig. 5. The cells were processed with JSHJ extract at a dose of 2, 20, and 50 μg/mL for 24 h. At all tested concentrations, the survival rate of RAW264.7 cells remained within (100 ± 10)%, indicating that the extract is non-cytotoxic. Therefore, the doses of 2, 20 and 50 μg/mL were designated as the low, medium, and high concentrations for subsequent experimental studies.

***Effects of JSHJ extract on NO generation in RAW264.7 cells***

To evaluate the anti-inflammatory action of the JSHJ extract, NO generation in LPS-exposed RAW 264.7 cells was monitored as described by Khumalo *et al* (Khumalo *et al*., 2024). We investigated NO production in RAW 264.7 macrophage cells, which were incubated at different concentration levels of the JSHJ extract (2, 20, and 50 μg/mL) for 2 h, and then exposed to 1 μg/mL LPS for 24 h. The NO levels within the medium were measured utilizing the Griess reaction. As illustrated in fig. 6, NO production in cells was markedly elevated in the LPS-stimulated model group versus the untreated group ($P < 0.01$). By contrast, NO production in the JSHJ extract-treated groups demonstrated a significant reduction ($P < 0.01$) as opposed to the LPS group, except for the low-dose concentration group. After treatment with JSHJ extract at the concentration level of 2, 20, and 50 μg/mL, NO levels decreased in a dose-responsive fashion. Notably, treatment with 50 μg/mL JSHJ-3 and JSHJ-4 significantly inhibited the overproduction of NO, reducing it from 9.45 umol/L to 0.86 and 0.16 umol/L, respectively.

***Influence of JSHJ extract on LPS-induced inflammatory cytokine release in RAW264.7 cells***

The anti-inflammatory effect of the JSHJ extract was further assessed by measuring the pro-inflammatory factor TNF-α. The impact of the JSHJ extract on the inflammatory reaction in RAW 264.7 cells activated by LPS was evaluated through experimentation. The cells were processed for 2 h with JSHJ extract at a dose of 2, 20, and 50 μg/mL, then exposed to LPS for 20 h. The experimental groups included a blank control group, a

JSHJ extract treatment group, an LPS-exposed group, and a PDTC positive control group. The cells were cultured in a 37℃ incubator, and the release of TNF-α in the supernatant of the cell cultures from each group was measured through ELISA analysis. As shown in fig. 7, TNF-α levels significantly increased from 8.089 to 127.26 pg/mL after 24 h of LPS treatment alone. Pretreatment with JSHJ extract at medium and high doses led to a notable decrease of TNF-α levels relative to the LPS-treated group.

***Effect of JSHJ extrac on LPS-Induced ROS levels***

To assess the effect of JSHJ extract on oxidative injury, the generation of ROS was measured in RAW 264.7 cells triggered with LPS. The cells were pre-exposed to a range of JSHJ extract (2, 20, 50 μg/mL) for 2 h, then exposed to LPS for 20 h. ROS production was quantified via a fluorescent probe, such as DCFH-DA, which reacts with ROS to emit fluorescence, providing a quantitative measure of oxidative stress.

The experimental groups included a blank control group, JSHJ extract treatment group, LPS stimulation group, and a positive control group (e.g., PDTC). After treatment, cells were incubated with the fluorescent probe, and Fluorescence levels were quantified with the aid of a microplate reader. The results are presented in fig. 8. LPS stimulation notably enhanced ROS generation in RAW 264.7 cells, as evidenced by the brightest intracellular green fluorescence. Compared to the PDTC group, fluorescence intensity was notably reduced in the JSHJ extract treatment groups, suggesting a marked decrease in ROS production. Importantly, all three concentrations of JSHJ extract significantly reduced fluorescence intensity and ROS production, indicating that JSHJ extract possesses antioxidant properties and may contribute to alleviating oxidative stress related to inflammation. However, the concentration that showed the most pronounced effect (50 μg/mL) was selected for presentation in fig. 8. These results suggest that JSHJ extract effectively scavenges LPS-induced intracellular ROS accumulation, with the strongest effect observed at 50 μg/mL for both JSHJ-1 and JSHJ-5.

## DISCUSSION

Harvesting and processing play an essential role in evaluating the quality of traditional Chinese medicine (Liu *et al*., 2024). Accurately determining the optimal harvesting time is of great significance for ensuring high quality, increasing yield, enhancing overall benefits, and reducing labor intensity. JSHJ is a widely used plant with both food and medicinal applications, and its optimal harvesting period must be scientifically determined to maximize both yield and quality.

The HPLC fingerprinting method is broadly implemented in TCM research due to its speed, precision, and high reproducibility (Bai *et al*., 2020). This study involved analyzing the HPLC fingerprints of JSHJ gathered at distinct time moments and quantifying the relative contents of 3,5-O-dicaffeoylquinic acid, chlorogenic acid, and galuteolin. Through a comparison of the HPLC fingerprints of nine different JSHJ batches, harvested at varying times and from several plant parts, we identified seven shared peaks, with similarity coefficients spanning from 0.592 to 1.000. These findings indicate marked differences in the chemical composition of JSHJ across multiple harvesting intervals.

Therefore, establishing a thorough profile of JSHJ at different harvesting times is critical, including the identification of its active ingredients and bioactive compounds, to inform cultivation, harvesting, processing, and efficacy studies. Significant fluctuations in the levels of three bioactive compounds-3,5-O-dicaffeoylquinic acid, chlorogenic acid, and galuteolin-were observed across nine JSHJ batches harvested at distinct time moments.The relative peak areas of each common peak, as shown in table 5, were calculated using the peak area of 3,5-O-dicaffeoylquinic acid as a reference. The relative content, derived from these peak areas, was highest at the SH stage, following the trend: SH > CH > ZH. By combining these results with JSHJ biomass factors, the SH stage was identified as the optimal harvesting period. Additionally, the research indicates that the green part of JSHJ is rich in chemical components, underscoring its potential for development and utilization.

This phytochemical optimization is particularly relevant given the growing need for natural anti-inflammatory agents. Inflammation is a complex series of physiological and pathological responses triggered by the body in reaction to external stimuli, such as infections caused by pathogenic microorganisms or tissue injury (Medzhitov, 2008). Excessive inflammation is linked to the onset of a variety of chronic health conditions, including sepsis, cancer, obesity, and inflammatory bowel disease (Marchi *et al*., 2022; Aksentijevich *et al*., 2020). These conditions present a significant challenge to society, as they not only impose a substantial economic burden but also contribute to a reduction in the average life expectancy of affected individuals (Utzeri and Usai, 2017). Therefore, inhibiting excessive inflammation is crucial for safeguarding overall health and preventing disease-related damage.

Currently, the anti-inflammatory drugs available on the market primarily include steroidal hormones and non-steroidal inhibitors. While these drugs are effective in reducing inflammation and alleviating pain, long-term use can lead to a range of adverse side effects (Granowitz and Brown, 2007). As a result, the search for new natural anti-inflammatory drugs to prevent and treat various diseases remains a vital area of research.

Through this work, we have elucidated the anti-

inflammatory effect of JSHJ extract. JSHJ is a traditional Chinese tea beverage with a long history, but there is limited literature on its phytochemical composition and associated biological activities. In particular, few investigations have centered on the anti-inflammatory effects of JSHJ extracts derived from various solvents. As an endotoxin, LPS is a fundamental element of the external membrane layer of Gram-negative bacteria and acts as a major trigger for initiating the microbial-driven inflammatory response. Macrophages are crucial in the course of inflammation and contribute significantly to the development of various immunopathologies. During inflammation, macrophages mediate the overproduction of pro-inflammatory substances, such as NO, TNF-α, and contribute to elevated levels of ROS (Xie *et al*., 2023; Park *et al*., 2022 ). LPS triggers the MAPK and NF-κB pathways initiation in macrophages, promoting the release of these inflammatory mediators (Xie *et al*., 2022). Among these mediators, NO is a central player in inflammation. TNF-α is a typical pro-inflammatory cytokine, and its excessive release is closely linked to the pathogenesis of inflammation. Therefore, inhibiting the overproduction of NO, TNF-α is a crucial strategy for reducing inflammation (Zhao *et al*., 2021).

This study sought to examine the impact of six JSHJ extracts (JSHJ-1 to JSHJ-6) on cell survival, NO production, and TNF-α levels in cells upon treatment with LPS as an inflammation model. These effects were assessed through MTT, Griess, and ELISA assays. The MTT assay indicated that the JSHJ extract did not exhibit any cellular toxicity on RAW264.7 cell. It was found that JSHJ extract exhibited a strong anti-inflammatory effect in the inflammatory environment triggered by LPS in RAW264.7 macrophages for the first time. The significant elevation in the discharge of pro-inflammatory mediators (NO and TNF-α) caused by LPS was notably reversed by pretreatment with JSHJ (20 and 50 μg/mL). Specifically, JSHJ-3 and JSHJ-4 showed the most significant activity, demonstrating their anti-inflammatory effects (Kwint *et al*., 2014).The inflammation-suppressing effect of JSHJ extract is primarily concentrated in the petroleum ether and ethyl acetate segments. Research has shown that the petroleum ether fraction (PEF) of the ethanolic extract of *Chrysanthemum morifolium* shows considerable anti-inflammatory potential in various animal models. For instance, PEF demonstrated a dose-dependent inhibition of inflammation in Xylene-induced ear edema assay and carrageenan-induced paw inflammation test, highlighting its therapeutic efficacy for inflammatory conditions (Yang *et al*., 2017). Moreover, the extract of ethyl acetate from *Chrysanthemum* has been investigated for its properties that reduce inflammation. It was observed to significantly prevent the release of pro-inflammatory mediators, including NO and PGE2, in LPS-treated RAW264.7 cells. The extract also inhibited the regulation of inflammatory gene expression like inducible nitric oxide synthase and TNF-α, thereby highlighting its role in modulating inflammatory responses (Guo *et al*., 2011). Overall, the concentration of anti-inflammatory activity in petroleum ether and ethyl acetate fractions of *Chrysanthemum* extracts underscores their significance in traditional medicine and their potential for development as effective anti-inflammatory agents (Chen *et al*., 2021).

ROS are key mediators of inflammation in vivo, primarily produced by NADPH oxidase. ROS function as secondary messengers in inflammation by activating downstream signaling cascades (Liu *et al*., 2024). They also contribute to the overactivation of the general immune response aimed at removing pathogens and healing damaged tissues (Shaukat *et al*., 2024). Studies have shown that LPS can stimulate ROS production (Chen *et al*., 2017; Kong *et al*., 2024). In this study, LPS stimulation of RAW264.7 cells caused a substantial increase in the levels of intracellular ROS after 20 h. However, all three concentrations of the JSHJ extract significantly reduced fluorescence intensity and decreased ROS production, among them, JSHJ-1 and JSHJ-5 concentrations of 50μg/mL had the most significant effect, indicating that JSHJ extract has antioxidant properties and may help mitigate oxidative stress associated with inflammation.

## CONCLUSION

The SH stage is the optimal harvesting period for JSHJ, with extracts, especially JSHJ-3 and JSHJ-4, demonstrating notable anti-inflammatory activity. These results highlight the potential of JSHJ extracts as natural agents for inflammation management.

## ACKNOWLEDGEMENTS

This study was supported by the Scientific Research Foundation for the Forestry Science and Technology Project of Guizhou Province (QLKH 2022-06), the Science and Technology department of Guizhou Province (QKHJC2024-640), and Special Research Project of Rural Economic Revitalization and Agricultural Industry Technology of Guizhou Medical University. The authors are grateful to Professor Qingde Long at Guizhou Medical University for the identification of *Chrysanthemum morifolium*.

***Conflict of interest***

The authors have no conflict of interest.

## REFERENCES

Aksentijevich M., Lateef SS, Anzenberg P, Bonora E and Zaug B (2020). Chronic inflammation, cardiometabolic diseases, and effects of treatment: Psoriasis as a human model. *Trends Cardiovasc. Med.*, **30**(8): 472-478.

Al Mamun A, Shao C, Geng P and Zhang J (2024).

Polyphenols targeting NF-κB pathway in neurological disorders: What we know so far? *Int. J. Biol. Sci.*, **20**: 1332-1345.

Abotaleb M, Liskova A, Kubatka P and Kajo K (2020). Therapeutic potential of plant phenolic acids in the treatment of cancer. *Biomolecules*, **10**(2):221.

Bai C, Yang J, Cao B, Xie T, Zhang Z and Zhang X (2020). Growth years and postharvest processing methods have critical roles on the contents of medicinal active ingredients of *Scutellaria baicalensis*. *Ind. Crops Prod*., **158**: 112985.

Chen L, Liu P, Feng X, Wang X and Li J (2017). Salidroside suppressing LPS-induced myocardial injury by inhibiting ROS-mediated PI3K/Akt/mTOR pathway in vitro and in vivo. *J. Cell Mol. Med.*, **21**(12): 3178.

Chen Z, Cheng S, Lin H, Zhang X and Li Y (2021). Antibacterial, anti-inflammatory, analgesic and hemostatic activities of *Acanthopanax trifoliatus* (L.) merr. *Food Sci. Nutr.*, **9**(4): 2191-2202.

Chen S, Liu J, Dong GQ, Xu ZS, Shi Y and Li LL (2020). Flavonoids and caffeoylquinic acids in *Chrysanthemum morifolium* Ramat flowers: A potentially rich source of bioactive compounds. *Food Chem*., **344**: 128733.

Fanaro GB, Marques MR, Calaza KDC, Rodrigues M and Souza A (2023). New insights on dietary polyphenols for the management of oxidative stress and neuroinflammation in diabetic retinopathy. *Antioxidants(Basel)*, **12**(6): 1237.

Guo D, Xu L, Cao X, Zhang Y and Li X (2011). Anti-inflammatory activities and mechanisms of action of the petroleum ether fraction of *Rosa multiflora Thunb. hips*. *J Ethnopharmacol.*, **138**(3): 717-722.

Granowitz EV and Brown RB (2007). Antibiotic adverse reactions and drug interactions. *Crit. Care Clin*., **24**(2): 421-442.

Kong LL, Sun P and Pan X (2024). Glycerol monolaurate regulates apoptosis and inflammation by suppressing lipopolysaccharide-induced ROS production and NF-κB activation in avian macrophages. *Poultry Sci*, **103**(8): 103870.

Kwint M, Conijn S, Schaake E, Slotman BJ and Verbakel WF (2014). Intra-thoracic anatomical changes in lung cancer patients during the course of radiotherapy. *Radiother Oncol.*, **113**(3): 392-397.

Khumalo GP, Nguyen T, Van Wyk BE and Dlamini SP (2024). Inhibition of pro-inflammatory cytokines by selected southern African medicinal plants in LPS-stimulated RAW 264.7 macrophages. *J. Ethnopharmacol.*, **319**(2): 117268.

Kim DY, Won KJ, Hwang DI, Lee YH and Lim JH (2022). Essential oil from *Chrysanthemum boreale* flowers modulates SNARE protein-linked mast cell response and skin barrier proteins and ameliorates atopic dermatitis-like lesions in mice. *Hortic. Environ. Biotechnol*, **63**: 287-298.

Li Q, Tan Y, Chen S, Wang Y and Zhou X (2021). Irisin alleviates LPS-induced liver injury and inflammation through inhibition of NLRP3 inflammasome and NF-κB signaling. *J. Recept. Sig Transd. Res.*, **41**(3): 294-303.

Li Y, Liu Y, Zhang X, Zhou Y, Wang Y and Zhang S (2019). Chemical compositions of *Chrysanthemum* teas and their anti-inflammatory and antioxidant properties. *Food Chem*, **286**: 8-16.

Liu X, Liang L, Cai G, Zhang Y and Sun H (2024). Multivariate approach to assess the bioactive compounds of *Atractylodes chinensis* (DC.) Koidz in different harvest periods. *J. Chromatogr. B.*, **1246**: 124298.

Liu TT, Liu PH, Peng CL and Geng NZ (2024). Chinese medicine to regulate intestinal bacteria in the treatment of atherosclerosis: A review. *Pak. J. Pharm. Sci*., **37**(6): 1599-1607.

Marchi S, Guilbaud E, Tait SWG and Sorrentino G (2022). Mitochondrial control of inflammation. *Nat. Rev. Immunol.*, **23**(3): 159-173.

Medzhitov R (2008). Origin and physiological roles of inflammation. *Nature*, **454**(7203): 428-435.

Ouyang HZ, Fan YQ, Wei SJ, Wu YZ, Zhang YL, Li XX and Wang ZG (2022). Study on the chemical profile of *Chrysanthemum (Chrysanthemum morifolium)* and the evaluation of the similarities and differences between different cultivars. *Chem. Biodivers*, **19**(14): e202200252.

Park MY, Ha SE, Kim HH, Lee SH and Kim YS (2022). Scutellarein inhibits LPS-induced inflammation through NF-κB/MAPKs signaling pathway in RAW264.7 cells. *Molecules*, **27**(12): 3782.

Qin D, Wang Q, Li H, Ma Y, Zhang H and Li L (2020). Identification of key metabolites based on non-targeted metabolomics and chemometrics analyses provides insights into bitterness in Kucha. *Food Res. Int*., **138**: 109789.

Shaukat A, Rajput SA and Ali M (2024). Therapeutic administration of Luteolin protects against *Escherichia coliderived* Lipopolysaccharide-triggered inflammatory response and oxidative injury. *Acta Trop*, **255**: 107236.

Utzeri E and Usai P (2017). Role of non-steroidal anti-inflammatory drugs on intestinal permeability and nonalcoholic fatty liver disease. *World J. Gastroenterol.*, **23**(22): 3954-3963.

Wang L, Xiong F, Yang L, Zhao D and Xu L (2020). A seasonal change of active ingredients and mineral elements in root of *Astragalus membranaceus* in the Qinghai-Tibet Plateau. *Biol. Trace Elem. Res*., **199**: 3950-3959.

Xie CQ, Wang SF, Cao MY, Zhang YJ, Li H and Liu ZM (2022). (E)-9-octadecenoic acid ethyl ester derived from lotus seedpod ameliorates inflammatory responses by regulating MAPKs and NF-κB signalling pathways in LPS-induced RAW264.7 macrophages. *Evid. Based Compl Alt.*, 6731360: 1-9.

Xie CQ, Wang SF, Lin XY, Zhang YJ, Li H and Liu ZM. (2023). Effect of n-hexane extract of *Camellia oleifera* fruit hull on inflammatory responses in LPS-induced

RAW264.7 cells. *J. Food Nutr. Res-Slov*., **11**(4): 301-309.

Xiong J, He J, Zhu J, Zhang L and Li Z (2022). Lactylation-driven METTL3-mediated RNA m6A modification promotes immunosuppression of tumor-infiltrating myeloid cells. *Mol Cell*, **82**(9): 1660-1677.

Yang WS, Kim D, Yi YS, Kim YS and Lee CW (2017). AKT-targeted anti-inflammatory activity of the methanol extract of *Chrysanthemum indicum var. albescens*. *J. Ethnopharmacol.*, **6**(201): 82-90.

Yang M, Tian X, Zhang M, Li Z and Chen Y (2022). A holistic comparison of flavor signature and chemical profile in different harvesting periods of *Chrysanthemum morifolium* Ramat. based on metabolomics combined with bioinformatics and molecular docking strategy. *RSC Adv*., **12**(54): 34971-34989.

Yuan H, Jiang S, Liu Y, Chen L and Yang J (2020). The flower head of *Chrysanthemum morifolium* Ramat (Juhua): A paradigm of flowers serving as Chinese dietary herbal medicine. *J. Ethnopharmacol*., **261**: 113043.

Zhao HK, Wu L, Yan GF, Zhang J, Li HJ and Li Y (2021). Inflammation and tumor progression: signaling pathways and targeted intervention. *Signal Transduct. Tar.*, **6**(1): 263.

Zhang Y, Li B and Wu G (2022). Dandelion (*Taraxacum mongolicum* Hand.-Mazz.) suppresses the decrease in physical strength and exercise capacity caused by insufficient liver function. *Appl Biological Chem*, **65**: 89.